A Numerical Study of NOx and Soot Emissions in Counterflow Methane/ n-Heptane Triple Flames

BY

PRITHVIRAJ SABNIS
B.E. Mechanical Engineering
University of Pune, 2013

THESIS

Submitted as partial fulfillment of the requirements
for the degree of Master of Science in Mechanical Engineering
in the Graduate College of the
University of Illinois at Chicago, 2015

Chicago, Illinois

Defense Committee:

Suresh K. Aggarwal, Chair and Advisor
Kenneth Brezinsky
Raghu Sivaramakrishnan, Argonne National Laboratory

This thesis is dedicated to my family

ACKNOWLEDGEMENTS

First and foremost, I would like to express my gratitude to God for blessing me with good health and capability to successfully complete my studies. Also I want to thank my parents and sister, for without their love and constant support I wouldn't have been able to make it to USA for my studies.

I would like to thank my advisor, Prof. Suresh K. Aggarwal for giving me an opportunity and his continued support and guidance throughout this work. His constant motivation inspired me to complete the research. I am thankful to Prof. Kenneth Brezinsky and Dr. Raghu Sivaramakrishnan for agreeing to be a part of my thesis committee.

I would also like to thank all my laboratory mates of Flow and Combustion Simulation Laboratory, especially Xiao Fu, who helped me with any obstacles I faced during my research. It was an enjoyable yet learning journey. Lastly I would like extend my gratitude to all my friends who were very supportive and made me feel at home in Chicago.

TABLE OF CONTENTS

LIST OF TABLES

LIST OF FIGURES

LIST OF FIGURES (Continued**)**

LIST OF FIGURES (Continued**)**

SUMMARY

There is significant interest in developing alternative and environmentally-friendly fuels with the objective of reducing global emissions and our dependence on conventional fuels. Both engine manufacturers and researchers have focused their efforts in using cleaner fuels, such as syngas and natural gas (NG), in transportation and power generation systems. In this work we report a computational study to investigate NO_x and soot emissions in n-heptane/methane triple flames in an opposed-jet configuration. The objective is to assess various fuel injection scenarios in a dual-fuel diesel engine using a simple configuration that can imitate partially premixed combustion in a diesel engine. Numerical simulations are performed by combining a detailed fuel and NO_x chemistry model with a soot model. Three fuel blending strategies are examined. In strategy 1, both fuels are introduced through the fuel nozzle, while in strategy 2, n-heptane is introduced from the fuel nozzle and methane from the fuel and oxidizer side nozzles, and in strategy 3, n-heptane and methane are introduced from the fuel and oxidizer nozzles, respectively. These three strategies represent different injection methods in a dual fuel diesel engine. The first strategy is similar to the condition when both methane and n-heptane are injected from the same nozzle or the nozzles are very close to each other. The second strategy represents the case where methane is injected into the cylinder first, mixed with air and then near the end of compression stroke, diesel is injected. The third strategy emulates the case where there are two separate nozzles for methane and n-heptane and they are away from each other. These are three of several possible injection strategies in a dual-fuel diesel engine which can be investigated in further detail in future for better performance of the diesel engine.

For each strategy, NO_x, PAH and soot emissions, and thermal efficiency are characterized by varying the energy content between the two fuels, while keeping the total energy input rate fixed. The most important difference between strategy 1 and other two strategies is that the flame formed with the first strategy is a double flame, whereas strategies 2 and 3 result in a triple flame. As n-heptane in the blend is reduced, the benzene emission index (EIBENZ) and soot emission decrease with all three strategies. However, the reduction is much more pronounced with strategies 2 and 3 compared to strategy 1. This shows that the flame structure plays an important role in the emissions. In addition, reducing n-heptane in the blend leads to higher efficiency with strategies 2 and 3, but lower efficiency with strategy 1. With regards to NO_x emission, results indicate an optimum fuel blending ratio corresponding to a minimum EINO for strategies 2 and 3. In contrast, for strategy 1, EINO increases monotonically as n-heptane in the blend is reduced. Thus strategy #1 yields higher NO_x, PAH and soot emissions, and lower efficiency compared to other two strategies, and is not recommended.

Nomenclature

a_g = Strain rate (s^{-1})

CH_4 = Methane

E = total input energy rate (KJ/s)

EINO = Emission Index for NO

EIBENZ=		Emission Index for Benzene
L	=	Distance between the nozzles (m)
M	=	Molecular weight (g/mol)
NC_7	=	n-heptane
Pyrene	=	$C_{16}H_{10}$
q	=	heating value of fuel (MJ/Kg)
V	=	Velocity (m/s)
Y	=	mass fraction
ρ	=	density (Kg/m^3)
$\dot{\omega}$	=	Rate of consumption/formation

1. INTRODUCTION:

1.1 **Motivation and Aim:**

The energy requirement has increased at a rapid rate all over the world. Diesel engines play a very important role in meeting the energy demand in the transportation and power generation sectors. According to the Independent Petroleum Association of America (IPAA) [1] diesel contributes to around 20% of the US petroleum use. For the rest of the world, this number goes up to 30% because of higher dependency of developing nations on traditional fuels. Diesel engsines are used in light duty vehicles, on-highway trucks, heavy duty trucks, construction industry, farming machineries, submarines, low, medium and high load power generation sets and other applications. This shows the importance of diesel in meeting the energy requirements. But the petroleum reserves are depleting at an alarming rate. BP [2] has provided an interesting update on the reserves saying, at the present production rate by the proven reserves the world has enough oil to last for around 53 years. According to Institute of Mechanical Engineers (IMechE), [3] at the present rate of consumption the world oil reserves will deplete in 40 years. This has led to the imperative need of finding alternatives for these fuels. Using a diverse mix of fuels and technologies can meet the ever increasing global energy need while assisting the shift to a lower emissions world. Further crude oil has shown a high amount of fluctuation in prices as illustrated by Figure1, which largely affects the economy of developing and non-oil producing nations where most of the crude oil is imported. The economy of developing nations is of more of a concern because they cannot meet the expense of the high investments in infrastructure for the use of renewable resources as an alternative.

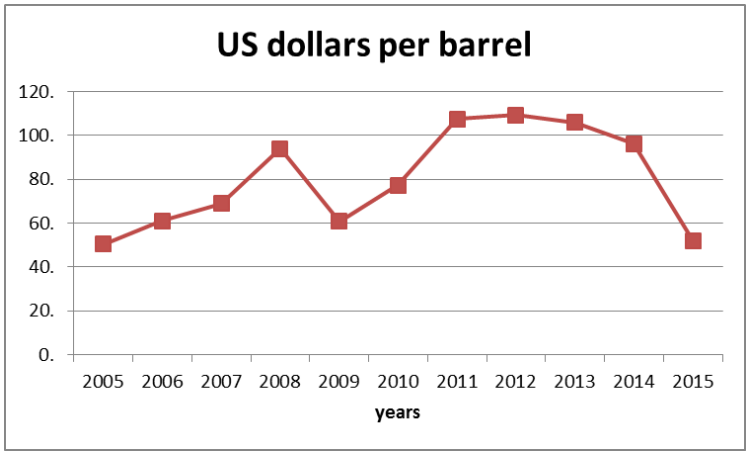

Figure 1: Fluctuation of the crude oil prices in last 10 years. Source: OPEC, IEA [4]

This induces a lot of instability. This provides another motivation for finding alternatives which will reduce the high dependency of nations on import of oil. A lot of studies have been carried out to test fuels which can be used with diesel like syngas, hydrogen, natural gas, biofuels etc. in a diesel engine. Diesel engines have a higher thermal efficiency and lower unburnt hydrocarbons and carbon monoxide (CO) emissions, hence are preferred over gasoline engines. In this present work the use of natural gas as an alternate fuel has been investigated in detail. According to the sustainability report 2014 by BP [2], natural gas is expected to contribute about 26% of the global energy requirement by 2035. This calls for a detailed analysis of the effect of addition of natural gas in a diesel engine. Also, methane which is the main constituent of the natural gas (~95%) can be produced by bacterial decomposition of organic waste which is abundant in nature and can be categorized as a renewable resource. This also reduces the dependency on import of natural gas and can be produced locally. But the combustion of these fuels lead to the production of toxic gases which degrade the environment and have adverse effects on the human life and the ecosystem. The exhaust gases usually consist of harmful gases like oxides of nitrogen (NOx), unburnt hydrocarbons, carbon dioxide and other gases. Because of

the serious threats that these gases pose, the government agencies are enforcing stringent norms to reduce the NOx and soot emissions all over the world. This serves as a strong motivation to study the NOx and soot emissions by combustion of natural gas and diesel.

A number of experimental studies have been reported [5][6][7], establishing the viability of using NG-diesel fuel blends in diesel engines. The effects of various parameters, such as fuel blending ratio, injection timing, EGR, and gaseous fuel-air equivalence ratio at different engine loads have been characterized. Recent studies on dual fuel blends [8][9] have reported a decrease in NOx and CO_2 emissions. While a number of aspects have been examined [10]–[12], relatively few computational studies have been reported on the fundamental processes associated with dual-fuel combustion and emissions [11] [13]. For instance, in a conventional diesel engine, fuel is injected near the top dead center (TDC), and ignition occurs in a fuel rich mixture, followed by heat release through a hybrid combustion mode, involving rich premixed combustion and diffusion combustion. In contrast, in dual-fuel diesel engine, a gaseous fuel-air mixture may be introduced through the intake valve, while the diesel fuel is injected and compression ignited. Consequently, depending upon the load and other conditions, the heat release in a dual-fuel engine would also involve a lean combustion mode with a propagating flame,[14] in addition to the premixed and diffusion combustion modes. A detailed investigation of the flame structure helps understand the combustion process in a better way and hence reduce the NOx and soot emissions.

The diesel fuel is a mixture of many long chain saturated hydrocarbons and aromatic compounds. In order to numerically simulate the flames it is required to find a surrogate fuel which would represent the diesel fuel. In this work, n-heptane is used as a surrogate for diesel. n-Heptane closely represents the properties of diesel and also the oxidation chemistry of n-heptane

is widely studied, hence serves as a good surrogate fuel for diesel. Methane is a good surrogate fuel for natural gas as it is the main constituent (~95%) of natural gas and also the oxidation chemistry is well studied.

This study deals with the formation of NOx and soot in n-heptane/methane triple flames in the counter-flow configuration, the effect of addition of methane to n-heptane on the NOx and soot emissions and different routes that lead to the formation of NOx in this flame. A lot of research has been done on partially premixed methane/air triple flames [15][16] and n-heptane/air triple flames [17]–[20]. There are many previous works which studied the formation of NOx in laminar co-flow flames, counter-flow double flames and triple flames [16][18]. But studies on structure and emission characteristics of n-heptane/methane triple flames have not been reported. This counter-flow n-heptane/methane partially premixed triple flame is of great importance because this configuration resembles the diesel engine in dual fuel mode and we can get results that mimic the real-life practical situations. This research also involves different strategies of blending methane with n-heptane and its effect on NOx and the soot emissions, flame structure and efficiency. These strategies indicate different methods of injecting diesel and natural gas into the engine cylinder. In this research the one dimensional CFD code; Chemkin [21] is used.

1.2 Natural Gas overview:

Natural gas is one of the most important sources of energy. In US about 25% of the energy comes from natural gas [22]. Most of this energy is used for domestic purpose like heating and cooking, industrial purposes, energy production and only a small percentage of it is used for transportation purposes. Natural gas is odorless, colorless and non-toxic gaseous

mixture of hydrocarbons and other gases. The composition of natural gas is given in Table 1 [22].

Component	Range (mole %)
Methane	87 - 97
Ethane	1.5 – 7
Propane	0.1 – 1.5
Iso-butane	0.01 – 0.3
Higher hydrocarbons	Trace – 0.1
Nitrogen	0.2 – 5.5
Carbon dioxide	0.1 – 1
Oxygen	0.01 – 0.1
Hydrogen	Trace – 0.02

Table 1: Composition of natural gas[22]

Natural gas is one of the safest and cleanest fuels. It has a high calorific value and compared to other fossil fuels has reduced emissions of harmful gases like oxides of nitrogen (NOx), soot, unburnt hydrocarbons, carbon dioxide, particulate matter and other gases. In the purest form natural gas almost consists of just pure methane. Natural gas is a fossil fuel and just as other fossils it is found underneath the earth's crust. But natural gas can also be produced by bacterial decomposition of organic waste. This type of gas is known as biogenic methane [22]. This is anaerobic decomposition near the surface of earth. An example of biogenic methane is the landfill gas. New technologies are being implemented which could use the large amount of natural gas produced by the decomposition of the landfill waste. Hence natural gas can be

categorized as a renewable source of energy. But the use of natural gas has some limitations because of which it has not been widely applied in practical applications. One of the major concerns is the storage of natural gas. For natural gas to be used in engines it has to be compressed at high pressures and stored raising some safety concerns.

1.3 Dual Fuel Diesel Engine:

There is a need to reduce the dependency on diesel fuel due to its depleting resources and high price fluctuations. Dual fuel diesel engines are one of the innovative ways to achieve this. The other fuel that is used with diesel is natural gas. It is a reasonable choice because of high availability of natural gas and also the great cost advantage it offers. Working of a dual fuel diesel engine is illustrated in Figure 2 [23]. The natural gas is mixed with the air stream into the intake manifold. The air-to-fuel ratio is lean. Then the diesel is sprayed into the cylinder and then the ignition takes place like in a conventional diesel engine. It gives comparable results to a diesel engine in terms of power output, torque produced and produces lesser emissions. This dual fuel engine cannot operate on 100% natural gas as the combustion of natural gas requires activation energy which is provided by the combustion of diesel. The amount of diesel required depends upon the load conditions. For the purpose of numerical simulations in this work, the total rate of energy input is kept constant which represents the load in a diesel engine and cases from 100% energy from n-heptane to 40% energy in n-heptane are considered and analyzed. This means up to 60% substitution of n-heptane by methane has been studied.

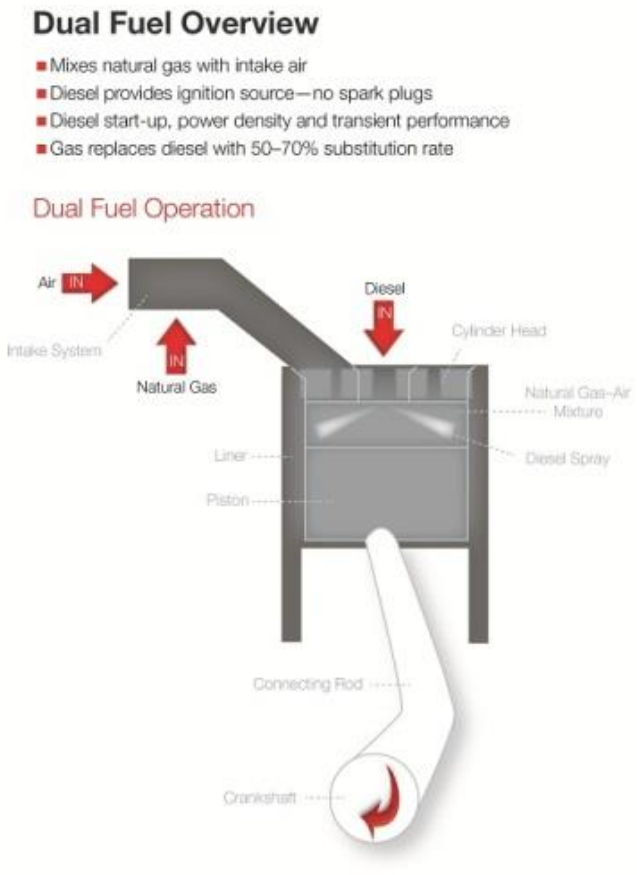

Figure 2: A schematic showing working of a dual fuel diesel engine[23]

1.4 Chemkin Overview:

Partially premixed flames are of pronounced importance because of its practical relevance in combustion systems like furnaces, gas turbines and diesel engines. Partially premixed flames are a combination of premixed and non-premixed flames hence it consists of multiple reaction zones. They can result in a double, triple or multiple flames.

The following section is taken from the Chemkin theory manual [21].

We use the opposed flow (counterflow) partially premixed flame and the OPPDIFF package [24]. In the opposed flow, we consider two jets from two concentric nozzles directed towards each other. For Chemkin, a steady-state solution is computed for axisymmetric flame between

two nozzles as shown in Figure 3. This configuration allows the flames to be flat and hence the flame chemistry and structure can be studied in detail. We assume that the radial velocity varies linearly with the radial direction, which leads to the simplification that the fluid properties are function of axial direction only.

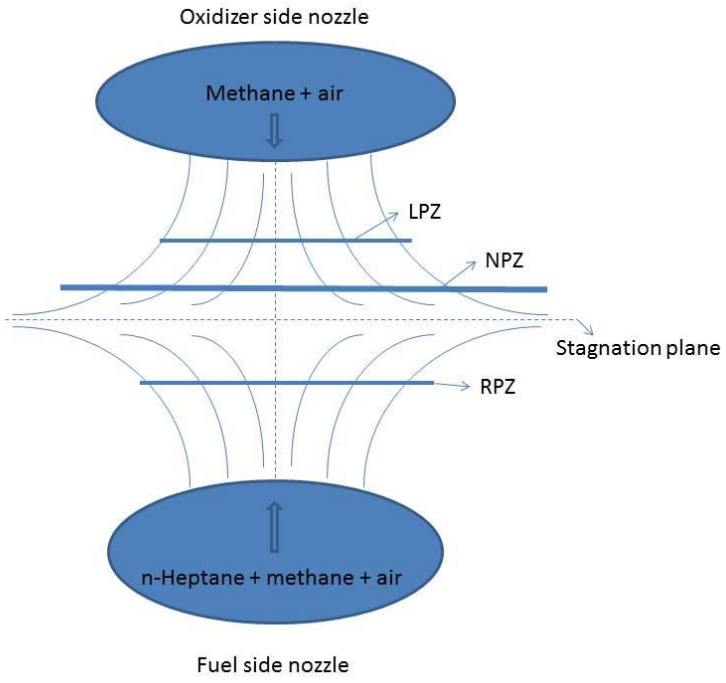

Figure 3: Schematic showing the configuration for the counter-flow flame set-up

The configuration discussed in Figure 3 results in a 2-D planar flow field with a stagnation plane between the two nozzles. The position of the stagnation plane depends on the momentum balance of the two streams. For a partially premixed flame it may result in two or three flames depending on the mixtures supplied from the two nozzles. If a premixed mixture of fuel and air is supplied from one nozzle and air from the other nozzle, it results in a double flame and if premixed mixture is supplied from both nozzles, a triple flame is established. The three flames are set up in the rich, lean and non-premixed zones (RPZ, LPZ and NPZ). The rich and

lean flames are formed as a result of combustion of the fuel supplied through the two nozzles. The non-premixed flame is formed when the excess oxygen reacts with the products of incomplete combustion. When the same mixture is supplied from opposite nozzle two identical flames are established known as twin flames which are used to calculate the flame speed. In this work we consider both double and triple flames. The flow simulator model is derived from a model which was formerly developed by Kee et. al. [25] for premixed opposing flows. The configuration as described in Fig. 3 helps to formulate the equations only along the axis thus reducing it 1-D system of equations. The governing equations are discussed below.

The conservation of mass equation is cylindrical coordinates is given by:

$$\frac{\partial(\rho u)}{\partial x} + \frac{1}{r}\frac{\partial \rho v_r r}{\partial r} = 0 \tag{1}$$

Where u denotes the velocity in axial direction, v_r denotes the velocity component in radial direction and ρ denotes the density. But Von Karman suggested that we can define the ρ and v_r/r should be a function of axial direction (x) only. Thus we can define:

$$G(x) = \frac{-(\rho v_r)}{r} \qquad F(x) = \frac{\rho u}{2} \tag{2}$$

Then using equation 2, the mass conservation equation reduces to:

$$G(x) = \frac{dF(x)}{dx} \tag{3}$$

We define an eigenvalue for perpendicular momentum as:

$$H = \frac{1}{r}\frac{\partial p}{\partial r} \tag{4}$$

Then using equation 4, we define the equation for conservation of momentum as:

$$H - (n-1)\frac{d}{dx}\left(\frac{FG}{\rho}\right) + \frac{nG^2}{\rho} + \frac{d\left[\mu\frac{d\left(\frac{G}{\rho}\right)}{dx}\right]}{dx} = 0 \qquad (5)$$

And the energy and species conservation equation is given by:

$$\rho u\frac{dT}{dx} - \frac{1}{C_p}\frac{d\left(\lambda\frac{dT}{dx}\right)}{dx} + \frac{\rho}{C_p}\sum_k C_{pk}Y_kV_k\frac{dT}{dx} + \frac{1}{C_p}\sum_k h_k\dot{\omega}_k + \frac{1}{C_p}\dot{Q}_{rad} = 0 \qquad (6)$$

$$\rho u\frac{dY_k}{dx} + \frac{d(\rho Y_kV_k)}{dx} - \dot{\omega}_kW_k = 0 \qquad \text{k = 1 ,……, K} \qquad (7)$$

Where Y, C_p, λ, h, $\dot{\omega}$ and Q_{rad} represents the mass fraction, specific heat, thermal conductivity, enthalpy, reaction rate and heat loss by radiation respectively. V_k is the diffusion velocity which is calculated by mixture averaged formulation given by:

$$V_k = -\frac{1}{X_k}D_{km}\frac{dX_k}{dx} - \frac{D_k^T}{\rho Y_k}\frac{1}{T}\frac{dT}{dx} \qquad D_{km} = \frac{1-Y_k}{\sum_{j\neq k}^{K}\frac{X_j}{D_{jk}}} \qquad (8)$$

Where D_{km}, D_{jk} and D_k^T are the mixture averaged, binary and thermal diffusion coefficients respectively.

We specify the boundary conditions as:

$$x = 0:\ F = \frac{\rho_F u_F}{2};\quad G = 0;\quad T = T_F;\quad \rho uY_k + \rho Y_kV_k = (\rho uY_k)_F \qquad (9)$$

$$X = L:\quad F = \frac{\rho_O u_O}{2};\quad G = 0;\quad T = T_O;\quad \rho uY_k + \rho Y_kV_k = (\rho uY_k)_O \qquad (10)$$

Where the subscripts F and O represent the fuel and oxidizer side nozzle respectively. The reaction rates are calculated using the chemical kinetics file which is provided to Chemkin. The reaction rates [26] are calculated using:

$$\dot{\omega}_k = \sum_{i=1}^{I} V_{ki} q_i \qquad (k = 1, \ldots\ldots, K) \tag{11}$$

Where:

$$V_{ki} = V''_{ki} - V'_{ki} \tag{12}$$

$$q_i = k_{fi} \prod_{k=1}^{K} [X_k]^{V'_{ki}} - k_{ri} \prod_{k=1}^{K} [X_k]^{V''_{ki}} \tag{13}$$

Where k_f and k_r are the reaction rates for forward and reserve direction respectively. [21]

2. NUMERICAL MODEL:

Simulations of triple flames are carried out using the OPPDIF code and the Chemkin package [24]. OPPDIF computes the flame structure in an opposed flow configuration, allowing evaluation of effects of the strain rate, partial premixing, fuel blending, and other parameters on various flames. Simulations account for thermal radiation through an optically thin model. The fuel oxidation chemistry is modeled using the Ranzi mechanism [27][28] which also includes the NO_x chemistry corresponding to the four NO_x formation routes, namely the thermal, prompt, intermediate N_2O, and NNH routes. The models for these routes are adopted from various sources [29]–[31]. The resulting mechanism for hydrocarbon oxidation from methane up to n-octane, and of NO_x formation consists of about 170 species and about 5000 reactions.

Processes considered in the soot model include nucleation, surface growth through coagulation and interaction with gaseous species, and oxidation. The reaction mechanism for fuel oxidation is capable of simulating the formation of PAHs up to pyrene ($C_{16}H_{10}$). Particle inception is then modeled via a nucleation reaction with two pyrene molecules. The nucleation reaction provides the particle inception rate, and defines the size and the surface coverage of the particle (or nucleus). Once a primary particle is formed, it can grow through surface reactions and coagulation, and also undergo oxidation. The coagulation process is modeled using Frenklach's method of moments approach [32], [33]. The soot model is combined with the fuel oxidation and NOx formation model.

For the numerical solution in Chemkin, the convective terms are discretized using the upwind or central-difference approximations, while the diffusive terms are discretized using the central-difference approximations. For computational efficiency, a nonuniform adaptive mesh,

based on the magnitudes of first and second derivatives, is employed to resolve the reaction zone and other regions of large gradients.

The following section is taken from Chemkin theory manual [21].

The algebraic equations thus obtained are solved by the TWOPOINT solver. TWOPOINT solves the system of equation using the damped modified Newton's algorithm. If the algorithm fails to converge during the iteration the initial guess will be modified by integration of the time-dependent version of the equations over a fixed number of time steps. This provides a guess which is closer to the steady state solution increasing the chances of convergence to the solution. If the algorithm still fails to converge TWOPNT takes additional time steps on the temporary solution to further improve the initial guess. Ultimately, the steady-state solution is reached [21].

Grid independence was established by performing simulations with increasingly finer grids and by changing GRAD and CURV parameters until no variation was observed between two grid systems. GRAD and CURVE values of 0.3 and 0.5 were used respectively. This choice of GRAD and CURVE values along with the number of initial grid points of either 6 or 9 leads to a total of about 120 points in the final solution. This gives a good resolution. Each simulation takes around 2-3 hours to converge. As discussed in the next section, simulations were carried out for a number of n-heptane/methane triple flames, including the base case of a n-heptane/air double flame. A strain rate of 100 s^{-1} is used for all flames. In all the simulations, the rich mixture is supplied from the fuel side nozzle and the lean mixture from the oxidizer side nozzle. In all the simulations the rich mixture is supplied from the left side and the lean mixture is supplied from the right side. This configuration and fuel mixing strategies simulate the dual-

fueled diesel engine conditions as discussed in the previous section on dual fuel diesel engines, Fig 2. To ensure that n-heptane remains in gaseous state, inlet temperature for fuel side nozzle is maintained at 400 K. The other inlet temperature is maintained at 300 K. The velocities of both the oxidizer and fuel side are determined by specifying the global strain rate [34] and matching the momentum flow rates of the fuel and oxidizer jets, as given by the following two equations:

$$a_g = \frac{2*V_o}{L} * (1 + \frac{|V_f|\sqrt{\rho_f}}{|V_o|\sqrt{\rho_o}}) \quad (14)$$

$$\rho_o * V_o^2 = \rho_f * V_f^2 \quad (15)$$

The subscripts f and o denote the fuel and the oxidizer sides, respectively.

Two strategies were devised to classify different cases[1] for this study which are as follows:

- Keeping the equivalence ratio fixed and varying the total rate of input energy
- Keeping the total rate of energy input constant and varying the equivalence ratio

In this work, we keep the total energy flow rate into the system constant, corresponding to a base case of n-heptane double flame with equivalence ratio of 2 and a global strain rate of 100 s^{-1}. The different cases are formulated by keeping this total energy flow rate constant and varying the energy content between n-heptane and methane fuels. In all the cases the global strain rate is kept constant at 100 s^{-1}. This strategy is chosen so that the total energy input rate which is a measure of load on engine can be kept constant and the effect of fuel blending strategies on the NO_x and soot emissions can be studied. Six cases corresponding to different energy contents between the two fuels are as shown in Table 2.

[1] In both the cases the global strain rate was kept constant.

Case	Heptane Energy Content	Methane Energy Content
1	100%	0%
2	80%	20%
3	60%	40%
4	40%	60%
5	20%	80%
6	0%	100%

Table 2: Six simulation cases based on the relative energy contents between the two fuels.

The boundary conditions are obtained by solving the set of following equations along with equations (14) and (15).

$$\rho_f = (Y_{NC7} * \rho_{NC7}) + (Y_{airF} * \rho_{air}) + (Y_{CH4F} * \rho_{CH4}) \quad (16)$$

$$n_{NC7} + n_{airF} + n_{CH4F} = 1 \quad (17)$$

$$\rho_o = (Y_{airO} * \rho_{air}) + (Y_{CH4O} * \rho_{CH4}) \quad (18)$$

$$n_{airO} + n_{CH4O} = 1 \quad (19)$$

$$\left(\rho_{NC7} * n_{NC7} * V_f * q_{NC7}\right) + \left(\rho_{CH4} * n_{CH4} * V_f * q_{CH4F}\right) + (\rho_{CH4} * n_{CH4} * V_O * q_{CH4O}) = E \quad (20)$$

$$\frac{\rho_{NC7}*q_{NC7}*n_{NC7}*V_F}{(\rho_{CH4}*q_{CH4}*n_{CH4F}*V_f)+(\rho_{CH4}*q_{CH4}*n_{CH4O}*V_O)} = r \quad (21)$$

$$\frac{n_{CH4F}}{n_{airF}} = \frac{n_{CH4O}}{n_{airO}} \quad (22)$$

Equations 16 and 18 give the mixture densities on the fuel and oxidizer side inlet. Equation 20 gives the total rate of input energy which is kept constant and Equation 21 denotes the ratio of the energy content in heptane to energy content in methane (r). In this study, we also keep the ratio of methane mole fraction to air mole fraction (or methane equivalence ratio) on both the fuel and oxidizer sides constant as shown in Equation 22. We have 9 unknowns and solving them we get all the required boundary parameters. We use Wolfram alpha [35] which is a computational software to solve these equations.

3. RESULTS AND DISCUSSIONS:

3.1 **Model Validation:**

Simulations of counterflow n-heptane non premixed flames and partially premixed flames (PPF) using the Ranzi mechanism have been extensively validated in our previous studies [36], [37]. The validation included comparison of temperature and major species profiles, as well as various hydrocarbon and aromatic (toluene and benzene) species profiles. Validations of the NO_x mechanism have been reported by Shimizu et al. [38] and Frassoldati et al. [39]. The soot model in the combined mechanism has also been validated by Fu et al. [40] using the soot measurements in ethylene diffusion flames. An additional validation is provided herein for a counterflow methane partially premixed flame using the measurements of Li and Williams [41]. Figure 4 compares the predicted and measured temperature and major species profiles for a flame established at an equivalence ratio ϕ=1.5 and a_g=50s^{-1}. There is fairly good agreement between the measurements and predictions. The measured double flame structure containing a rich premixed reaction zone (RPZ) and a nonpremixed reaction zone (NPZ) are well predicted by the model. The locations of these reaction zones are also well captured by the model. The RPZ is located on the fuel side at about 4 mm from the stagnation plane, while the NPZ is located near the stagnation plane.

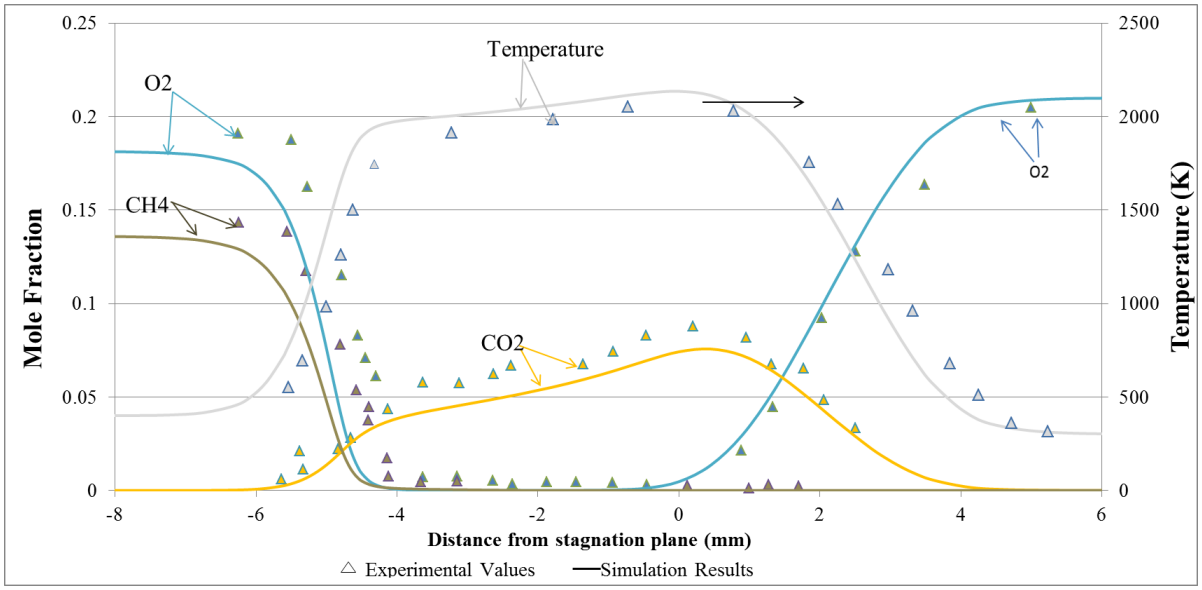

Figure 4: Predicted (lines) and measured (symbols) temperatures and major species (O_2, CH_4, CO_2) profiles in a methane partially premixed flame with φ=1.5 and a_g=50s^{-1} [41].

3.2 **Flame Structure for a Representative Dual-Fuel Case**

The computed flame structure for a representative n-heptane/methane triple flame is presented in Figures 5 and 6. For this flame, the rich and lean equivalence ratios (ϕ_r and ϕ_l) at the left and right nozzles are 1.8 and 0.18, respectively. The mixture in the left nozzle contains both n-heptane and methane fuels, while the right nozzle contains only methane fuel. This arrangement is made to create dual-fuel diesel engine like conditions.

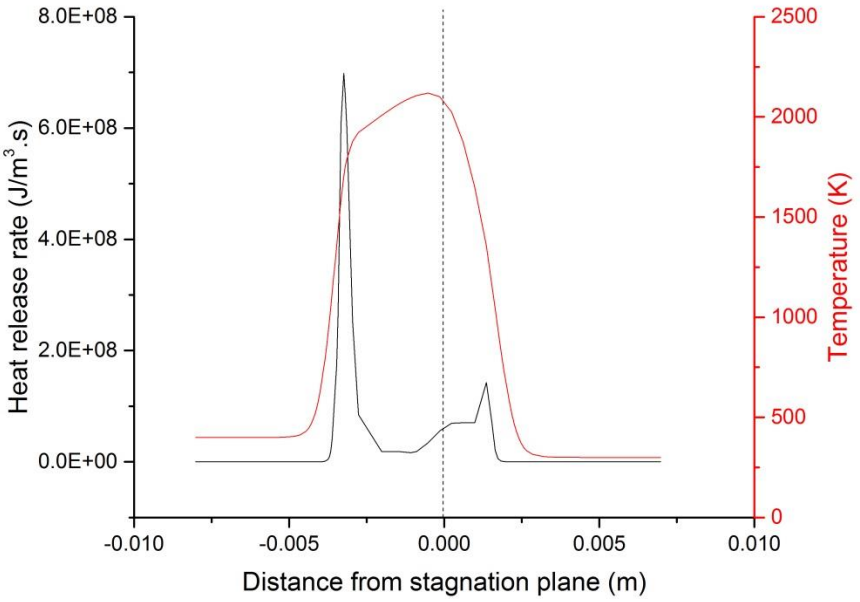

Figure 5: Heat release rate and temperature profiles plotted versus distance from the stagnation plane for a n-heptane/methane triple flame with 80% energy content in n-heptane (NC7), and strain rate of 100 s^{-1}. The vertical dashed line corresponds to the stagnation plane. The color of the plots and axes are matched.

The heat release rate profile in Fig. 5 shows three distinct peaks, which represent the locations of RPZ, NPZ, and LPZ (lean premixed reaction zone), respectively. The RPZ is formed by the oxidation of n-heptane and methane on the fuel side of the stagnation plane, while the LPZ is formed form the oxidation of methane on the oxidizer side. Fuels are completely consumed in the RPZ and LPZ. The diffusion flame is established by the burning of the incomplete products of combustion like CO, H_2, etc. formed in the RPZ and LPZ with the excess oxygen. It can be seen from Fig. 5 that the NPZ is located near the stagnation plane. The peak temperature is also found in this region. Figure 6 shows the temperature and major species profiles in the flame. It is seen that the intermediate combustion product species like H2, CO etc.,

are produced in the RPZ, and consumed in the NPZ. In addition, while both fuels from the fuel side nozzle get consumed in the rich premixed zone, n-heptane is consumed earlier compared to methane, since methane has a longer ignition delay (poor ignitability) than n-heptane. The energy required for methane to start igniting is high. N-heptane first gets burnt releasing some energy which is used by methane for its combustion. Therefore n-heptane is consumed first followed by methane.

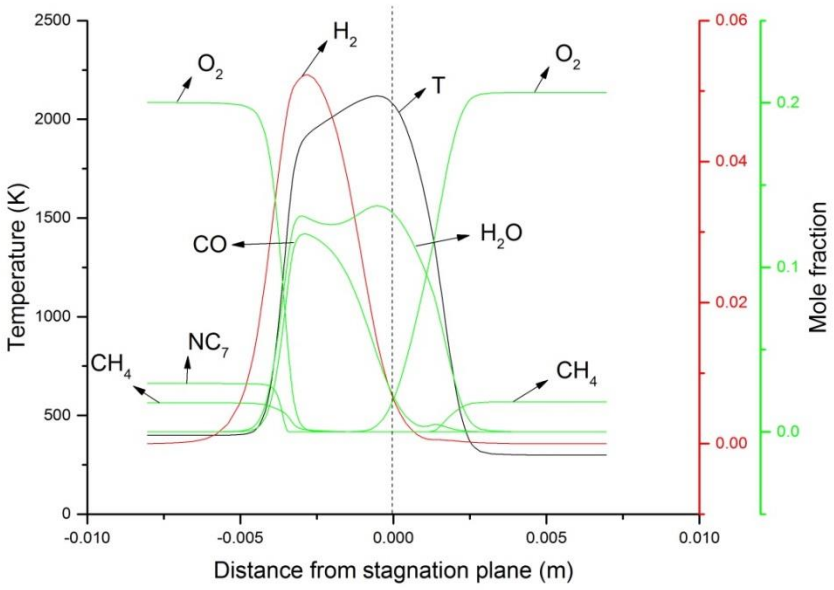

Figure 6: Temperature and major species mole fraction profiles plotted versus distance from the stagnation plane for the n-heptane/methane triple flame presented in Figure 1. The colors of the plots and axes are matched. The dashed vertical line corresponds to the stagnation plane.

Figure 7 presents the flame structure in terms of heat release rate profiles for three dual-fuel cases corresponding to 80%, 60%, and 40% energy content in n-heptane. Table 3 lists the

various parameters used for the simulation cases. In this work we limit the dual-fuel cases corresponding to a minimum energy content of 40% in n-heptane, since with further decrease, the equivalence ratio in methane-air stream gets close to 1 and the lean premixed reaction zone is formed right at the right nozzle, with significant heat loss there.

Case (Ref. Table 1)	Total energy input rate (MJ/s)	Rich side equivalence ratio	Lean side equivalence ratio
1	2.10257	2.00	0.00
2	2.10257	1.80	0.18
3	2.10257	1.60	0.36
4	2.10257	1.39	0.55

Table 3: The energy input rate and the equivalence ratios for the cases used for simulation.

A zoomed view of the region containing NPZ and LPZ is shown in Fig. 7b. As the energy content in n-heptane is reduced, the mixture equivalence ratio (ϕ_r) in the fuel nozzle decreases (less rich), while that in the oxidizer nozzle (ϕ_l) increases. Consequently, both the RPZ and LPZ become increasingly stronger, while the NPZ gets weaker, since the concentrations of the incomplete combustion products (CO, H_2, etc.) in the RPZ are reduced. This is because as the equivalence ratio becomes close to 1, a mixture closer to stoichiometric ratio is supplied which leads to complete combustion of the fuel. Figure 7 further indicates that with the reduced energy content in n-heptane, both the RPZ and LPZ move away from the stagnation plane, i.e., the

separation between them increases or the triple flame become wider, since the flame speeds for both the mixtures increase.

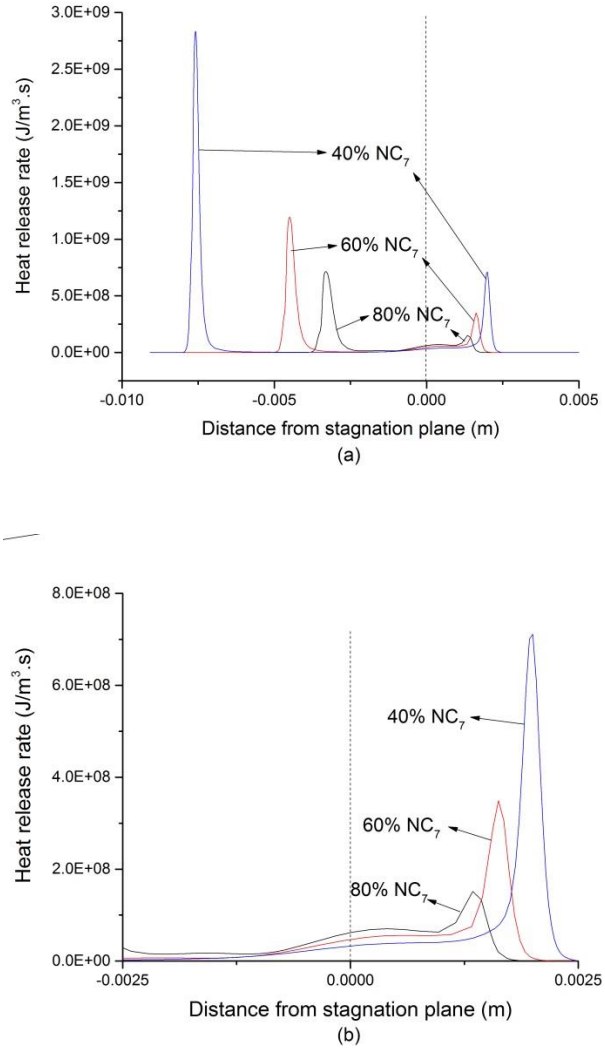

Figure 7: (a) Flame structures depicted in terms of heat release rate profiles with respect to the stagnation plane for three dual-fuel cases corresponding to 80%, 60%, and 40% energy content in n-heptane. A zoomed view of the region containing NPZ and LPZ is shown in Fig. 7b.

Figure 8 presents a comparison of the dual-fuel case (80% energy content in n-heptane) with the base case (with 100% energy content in n-heptane), the latter representing the

conventional diesel engine combustion. In conventional diesel there is no methane present. The air is taken into the cylinder at the suction stroke and then it is compressed followed by injection of diesel. Then the diesel is combusted because of the high temperature and pressure in the cylinder. This represents the case of double flame where a mixture of n-Heptane is supplied from the fuel side nozzle and air from the oxidizer side nozzle. As expected, there is a noticeable difference between the flame structures. The base case results in a double flame containing a RPZ and a NPZ, whereas the addition of methane produces a triple flame. Moreover, for the dual-fuel case, the n-heptane gets consumed earlier compared to the base case, i.e., the RPZ moves closer to the fuel nozzle, since the equivalence ratio of the rich mixture decreases which increases the flame speed, as mentioned earlier.

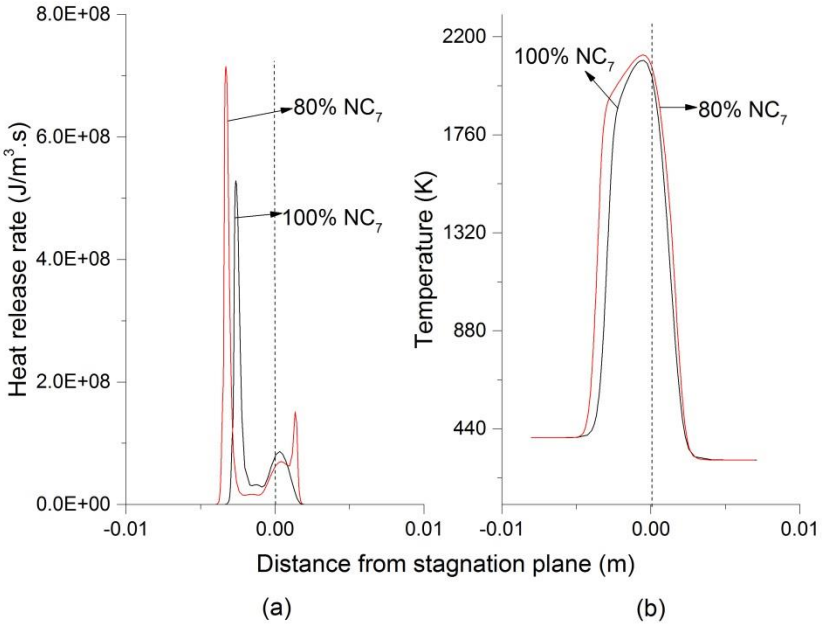

Figure 8: Comparison of double (base case) and triple flame (dual-fuel case) structures in terms of heat release rate (a) and temperature (b) profiles for a strain rate of 100 s^{-1}. The dashed line vertical represents the stagnation plane.

Then we study the effect of methane addition on the NOx and soot emissions. Figures 9 and 10 depict the effect of methane addition on soot and NO_x emissions for the various partially premixed flames discussed above. Figure 9 compares the benzene and NO mole fraction profiles for the double and triple flames discussed in the context of Fig. 8. There is no notable difference in the amount of NO being produced, although the peak value of NO decreases slightly for the dual-fuel case or triple flame compared to the double flame. However, the benzene formation reduces considerably with addition of even a small amount of methane.

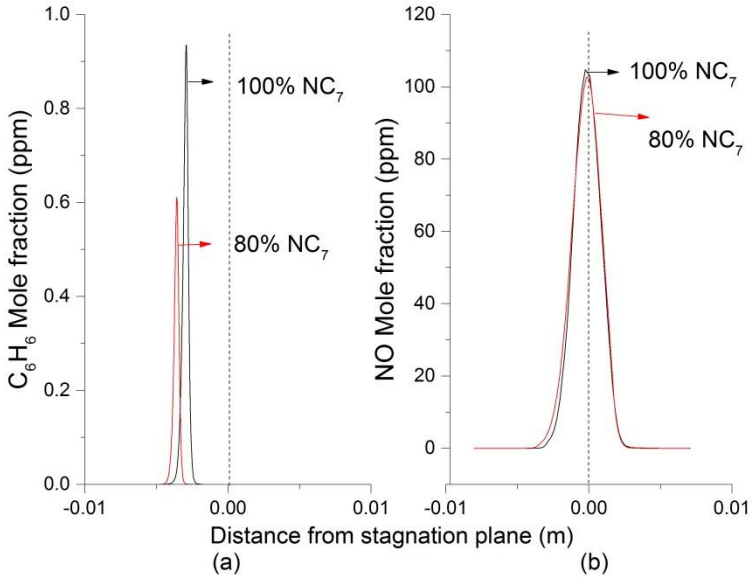

Figure 9: Mole fraction profiles of (a) benzene (C_6H_6) and (b) NO for the two partially premixed flames discussed in the context of Fig. 8. The dashed vertical line represents the stagnation plane.

Benzene is considered to be one of the most important precursors for soot formation and it is well known that heptane produces more benzene and therefore soot compared to methane. Methane is the smallest member of the hydrocarbon family. Benzene is an aromatic compound consisting of 6 carbon atoms. N-heptane in the seventh member of hydrocarbon family

consisting of 7 carbon atoms. Therefore n-heptane has to undergo lesser reactions to form benzene as compared to methane. The formation of benzene depends on the molecular structure of the fuel but when compared to methane, n-heptane produces more benzene. Thus, the addition of methane would lead to significantly lower soot emissions. It is also interesting to note that the benzene and thus soot is formed in the region near the RPZ, while the NO_x is formed in the NPZ where the temperature is the highest.

Figure 10 presents benzene and NO mole fraction profiles for n-heptane/methane triple flames corresponding to 80%, 60%, and 40% energy content in n-heptane. The temperature profiles for the three flames are also shown. As the fraction of methane in the blend is increased, it causes a significant reduction in benzene formation. Also with methane addition, the benzene formation region shifts toward the fuel nozzle, which is consistent with the movement of the rich premixed zone (RPZ) discussed earlier. Since with increasing methane addition, benzene is formed in a region with lower residence time, the amount of soot formed is reduced further. Figure 10 further indicates that with increasing methane addition, the NO formation zone becomes broader, since the high temperature region becomes wider.

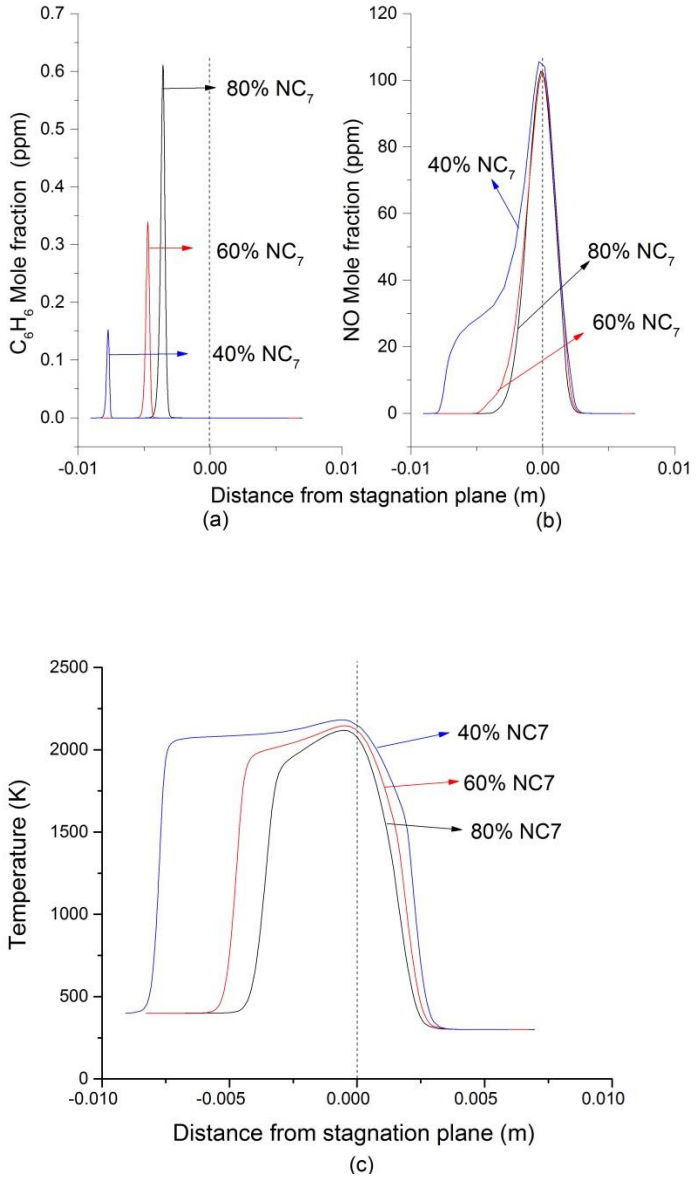

Figure 10: Mole fraction profiles of (a) benzene, (b) NO, and (c) temperature for three n-heptane/methane triple flames (discussed in the context of Fig. 7) corresponding to 80%, 60%, and 40% energy content in n-heptane. The dashed vertical line represents the location of stagnation plane.

However, the peak NO mole fraction, which is located in the NPZ, remains essentially the same for the three flames.

A global and perhaps better comparison of the emission characteristics for different fuel blends is provided by the NO emission index, defined as:

$$EINO = \frac{\int_0^L M_{NO}\dot{\omega}_{NO}dx}{-\int_0^L M_{fuel}\dot{\omega}_{fuel}dx} \quad (23)$$

Here M represents the molecular weight, $\dot{\omega}$ the net reaction rate (mol cm^{-3} s^{-1}), L the separation distance between the two nozzles, and x the axial coordinate. The benzene emission can be characterized similarly by defining a benzene emission index (EIBENZ). The effect of methane addition on NO and emission is shown in Figure 11, which plots the EINO and EIBENZ versus the n-heptane energy content. The variation of thermal efficiency, which is defined as the ratio of total heat release rate to the total energy input rate, is also shown in the figure. As the total energy input rate is kept constant in this study, we can compare the heat release rate for the different cases and define efficiency. Results indicate that with the increase in methane addition, the EINO varies in a relatively narrow range (within 12%). In contrast, there is a steep drop in EIBENZ as the amount of methane in the blend is increased. This is consistent with the benzene profiles presented in Figs. 9 and 10. It is also interesting to note that the addition of methane leads to a significant increase in thermal efficiency. This is due to the fact that the flame becomes broader, i.e., the heat release occurs over a wider region (cf. Fig. 7), as the amount of methane in the blend is increased.

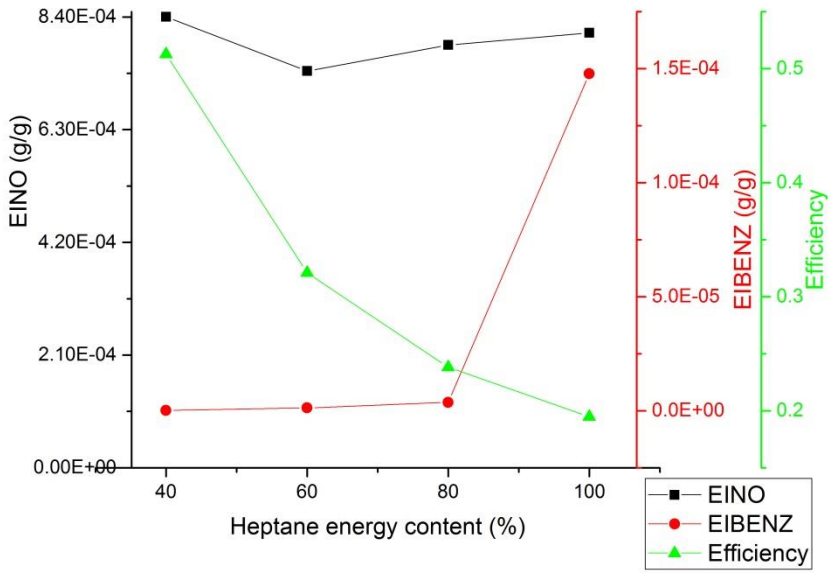

Figure 11: NO_x emission index (EINO), benzene emission index (EIBENZ) and thermal efficiency plotted versus the n-heptane energy content for n-heptane/methane triple flames with a strain rate of 100 s^{-1}. The colors of the plots and axes are matched.

The preceding results indicate a significant reduction in PAH emission with the addition of methane. As a consequence, one can expect a similar reduction in particulate emission with methane addition. The soot formation processes for the n-heptane/methane triple flame (with 80% energy in n-heptane) are depicted in Figure 12, which plots the profiles of O_2 and $C_{16}H_{10}$ (pyrene), soot volume fraction (f_v), particle number density (N_s, cm^{-3}), and average particle diameter (d_p, nm). The formation of PAH (pyrene) starts in the RPZ zone where the fuel (n-heptane & methane) pyrolysis occurs. Pyrene reaches its peak just after the RPZ and then it decreases gradually. As pyrene mole fraction decreases, nucleation is initiated, and soot particle number density increases. The particle diameter and soot volume fraction increase

simultaneously due to coagulation and surface reactions. The amount of soot formed continues to increase in the region between RPZ and NPZ, as there is no oxygen present in this region to oxidize the soot. However, near the stagnation plane some oxygen diffuses from the lean side. As a consequence, the soot oxidation is initiated, and the particle number density, particle size, and soot volume fraction decrease rapidly decrease beyond the stagnation plane. Thus the soot formation starts near the RPZ, and soot continues to form between RPZ and NPZ, and gets oxidized near the stagnation plane where the temperature is highest.

The effect of methane addition on soot emissions in triple flames is presented in Figures 12 and 13. Figure 13 compares the soot properties for two PPFs, i.e., a double flame with 100% energy in n-heptane and a n-heptane/methane triple flame with 80% energy in n-heptane. As indicated, the addition of methane leads to a significant reduction in the particle number density and the soot volume fraction. The peak values of number density and soot volume fraction decrease by a factor of 20 or more. Thus a relatively small amount of methane addition can cause a noticeable decrease in soot emission, although the region where the soot is formed remains essentially the same. As discussed earlier the soot production starts after the RPZ ends and all the soot is consumed or oxidized before the stagnation plane.

Figure 14 plots the soot properties for three n-heptane/methane triple flame with 80%, 60%, and 40% energy in n-heptane. As indicated, with increasing amount of methane addition, there is a drastic reduction in soot emission. For the flame with 40% energy content in n-heptane, there is essentially zero soot emission. This reduction in soot can be correlated to the reduction in PAH species, as clearly indicated in Figure 15, which compares the pyrene mole fraction profiles for the same three triple flames. As the energy in n-heptane is decreased from 80% to 40%, the peak pyrene mole fraction is reduced by two orders of magnitude. This is evident from earlier

benzene profile (c.f. Fig 10). Most of the pyrene is formed through benzene and thus the pyrene profile show similar behavior as shown in Fig 10a.

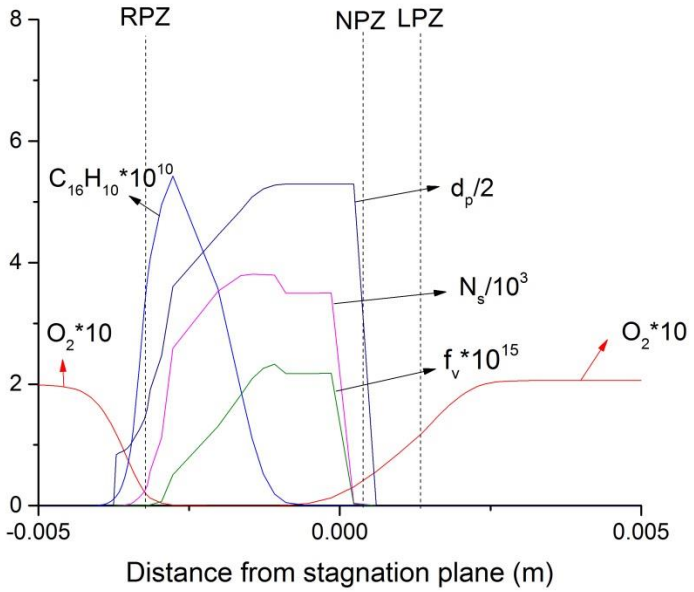

Figure 12: Soot formation processes in n-heptane/methane triple flame (with 80% of the energy content in n-heptane) at a strain rate of $100s^{-1}$. Figure shows the profiles of O_2 and $C_{16}H_{10}$ (pyrene), soot volume fraction (f_v), particle number density (N_s, cm^{-3}), and average particle diameter (d_p, nm). The vertical dashed lines represent the rich, lean and non-premixed zones.

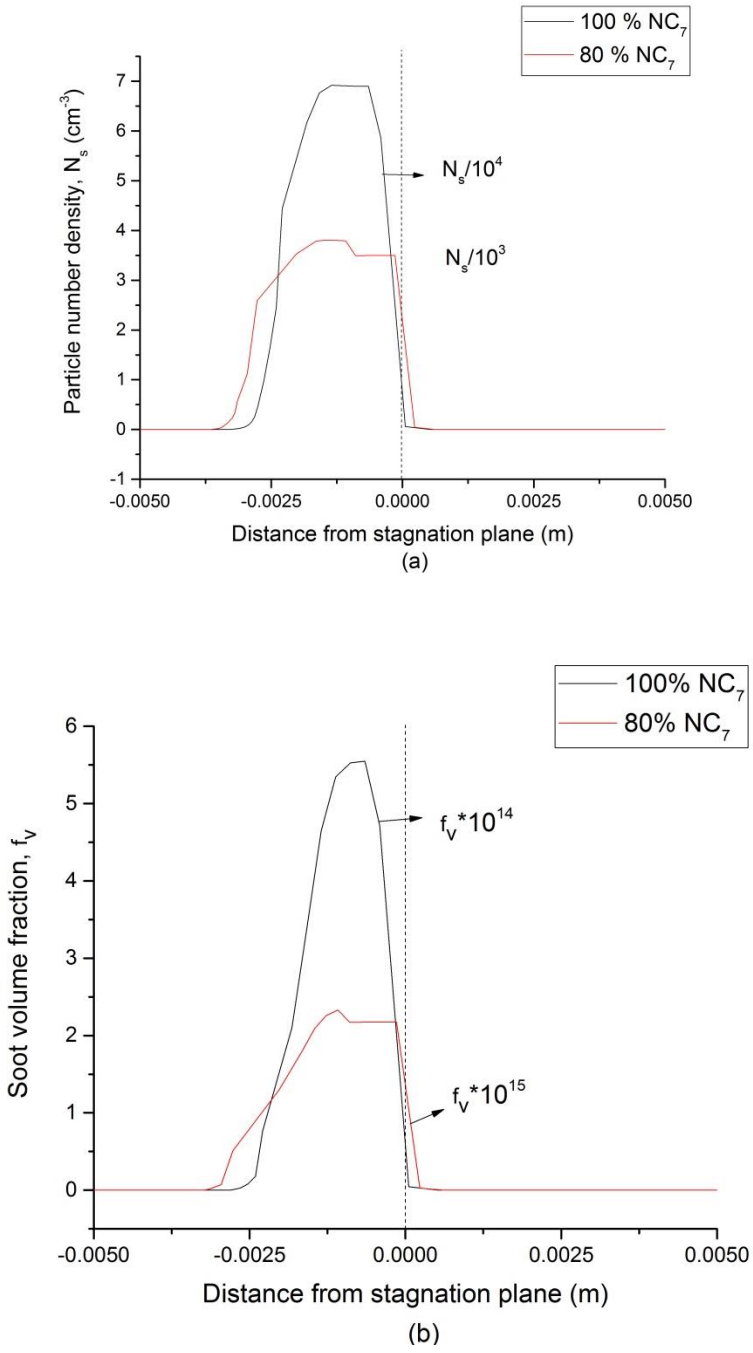

Figure 13: Comparison of particle number density (N_s) and soot volume fraction (f_v) for the n-heptane double flame (base case) and n-heptane/methane triple flame (dual fuel case with 80% energy in n-heptane). The vertical dashed line represents the stagnation plane.

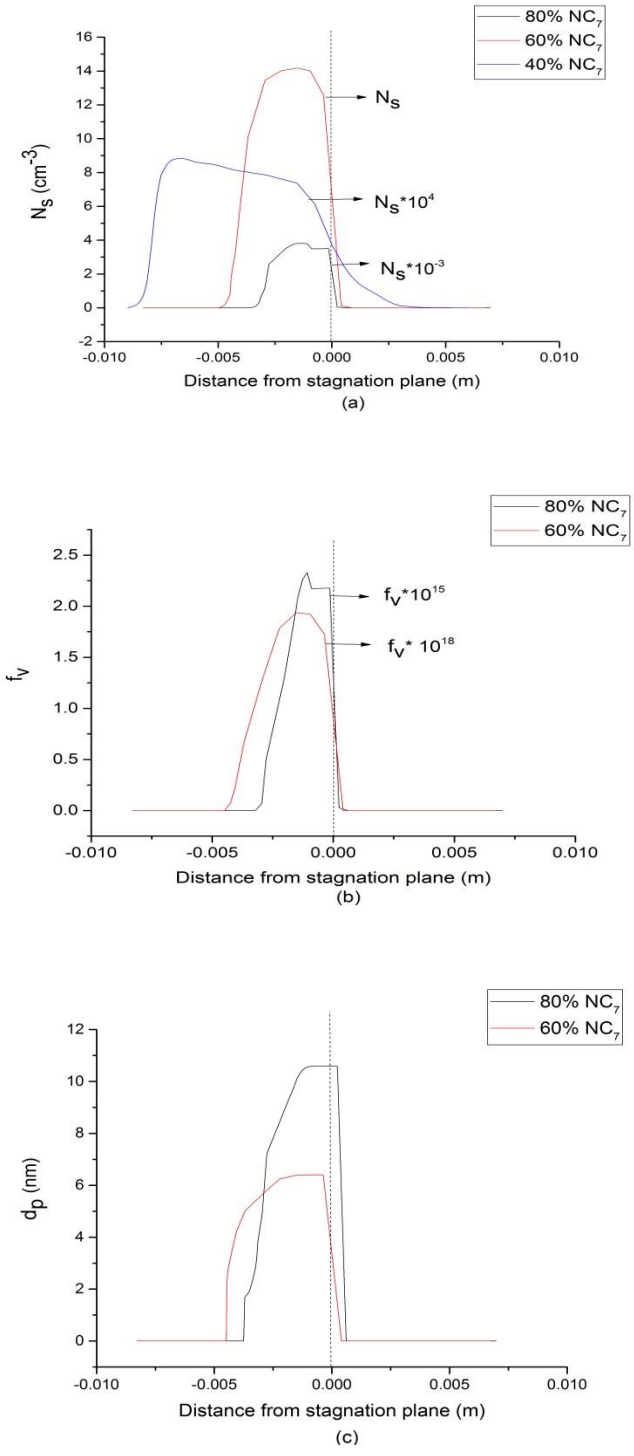

Figure 14 (a) particle number density (N_s), (b) Soot volume fraction (f_v), and (c) average particle diameter (d_p) for three n-heptane/methane triple flames corresponding to 80%, 60%, and 40% energy content in n-heptane. The dashed vertical line represents the location of stagnation plane.

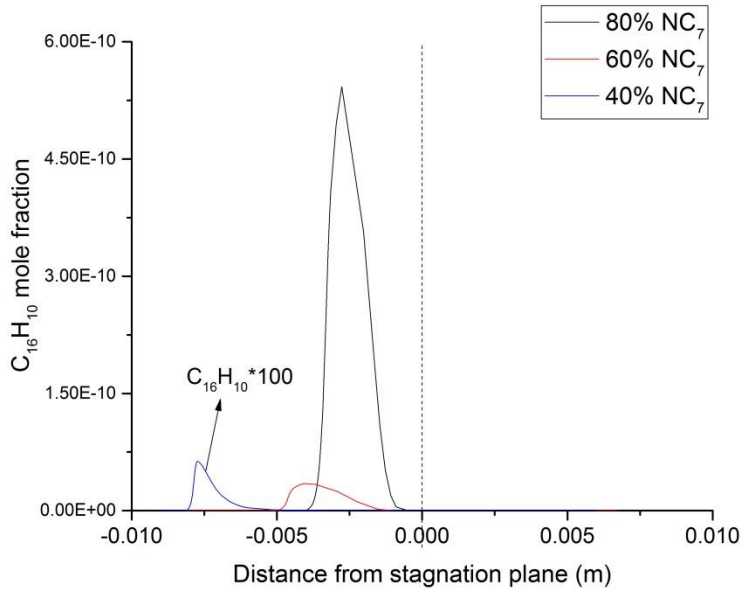

Figure 15: Pyrene ($C_{16}H_{10}$) mole fraction for three n-heptane/methane triple flames corresponding to 80%, 60%, and 40% energy content in n-heptane. The dashed vertical line represents the location of stagnation plane.

3.3 Effect of Methane addition on various NO Formation Routes

It is well established that NO_x formation in hydrocarbon flames is associated with four routes, namely the thermal, prompt, NNH intermediate and N_2O intermediate routes [15][17] [36][37]. In order to compute the contribution of a given NO formation route, we perform flame simulations by removing key reactions for the other three routes.

The following section is taken from Fu et. al. [37]

For instance the reactions for the thermal route are:

$$N_2 + O \rightarrow N + NO \quad (24)$$

$$N + OH \rightarrow NO + H \quad (25)$$

$$N + O_2 \rightarrow NO + O \quad (26)$$

From the above equations the initiation equation for thermal NOx is given by Eqn. 24.

Similarly the key reactions associated with prompt NO are:

$$CH + N_2 \rightarrow HCN + N \quad (27)$$

$$CH_2 + N_2 \rightarrow HCN + NH \quad (28)$$

$$C + N_2 \rightarrow CN + N \quad (29)$$

$$NH_2 + N \rightarrow N_2 + H + H \quad (30)$$

$$NCO + N \rightarrow N_2 + CO \quad (31)$$

$$N_2O + CO \rightarrow N_2 + CO_2 \quad (32)$$

$$NCO + NCO \rightarrow CO + CO + N_2 \quad (33)$$

$$NCO + NO \rightarrow N_2 + CO_2 \quad (34)$$

The reactions which are responsible for the N_2O intermediate mechanism are:

$N_2 + O + M \rightarrow N_2O + M$, $N_2O + H \rightarrow N_2 + OH$, $N_2O + O \rightarrow N_2 + O_2$, and $N_2O + OH \rightarrow N_2 + HO_2$

And lastly the reactions associated with the NNH sub mechanism are:

NNH→ N_2 + H, N_2 + H→ NNH + H, NNH + OH→ N_2 + H_2O, NNH + O_2→ N_2 + HO_2, NNH + O_2→ N_2 + H +O_2, NNH+ NH→ N_2 + NH_2, NNH + NH_2→ N_2 + NH_3, NNH + NO→ N_2 + HNO, HNNO + M → N_2 + OH + M, NH + N→ N_2 + H and NH + NO→ N_2 + OH [37].

Thus four sets of simulations are performed to compute the contribution of each NO route. Figure 16 compares the contribution of the four routes for two dual-fuel flames with 80%, and 60% energy content in n-heptane. For the flame with 80% energy in n-heptane, the thermal NO is the major route for NO formation, followed by the N_2O intermediate, prompt and NNH mechanisms. As the amount of methane is increased, the contributions of thermal NO and N_2O routes decrease, while that of prompt NO increases, and that of NNH route remains nearly the same.

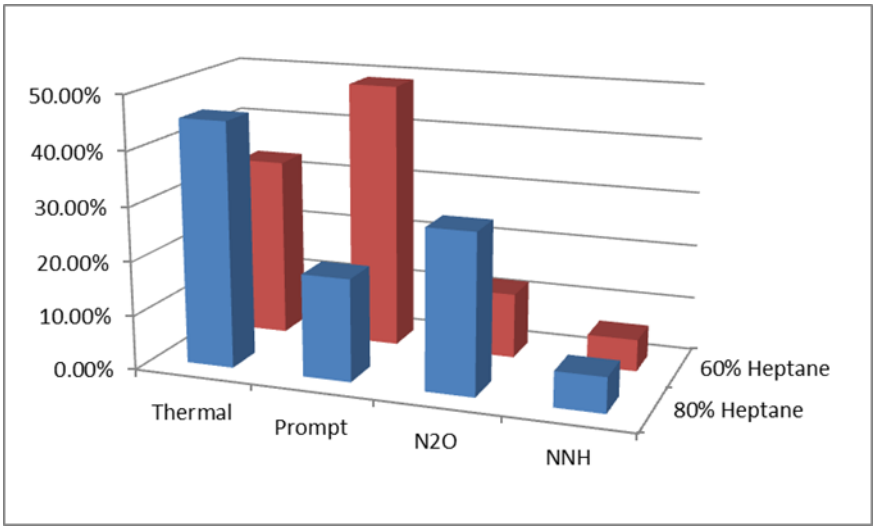

Figure 16: Contribution of the four NO formation routes for two cases of different heptane energy content of a n-heptane/methane triple flame for a strain rate of 100 s^{-1}.

In order to gain further insight, we plot in Figure 17 the variation of HCN and CH which are the main species associated with the prompt route. Results are shown for the three dual-fuel flames. The corresponding plot for N_2O is presented in Fig. 17c. As indicated in Fig. 17, as the amount of methane in the blend is increased, HCN formation is reduced but there is a sharp rise in CH formation, which leads to higher prompt NO.

Results in Fig. 14c indicate that the peak N_2O mole fraction decreases as the amount of methane is increased. Consequently, the contribution of N_2O intermediate route to total NO decreases with the increase in methane addition, as indicated in Fig. 13. It is also important to note that N_2O is mostly formed in the lean premixed reaction zone (LPZ), and as the amount of methane is increased, the equivalence ratio for the LPZ increases, which leads to a reduction in N_2O formation.

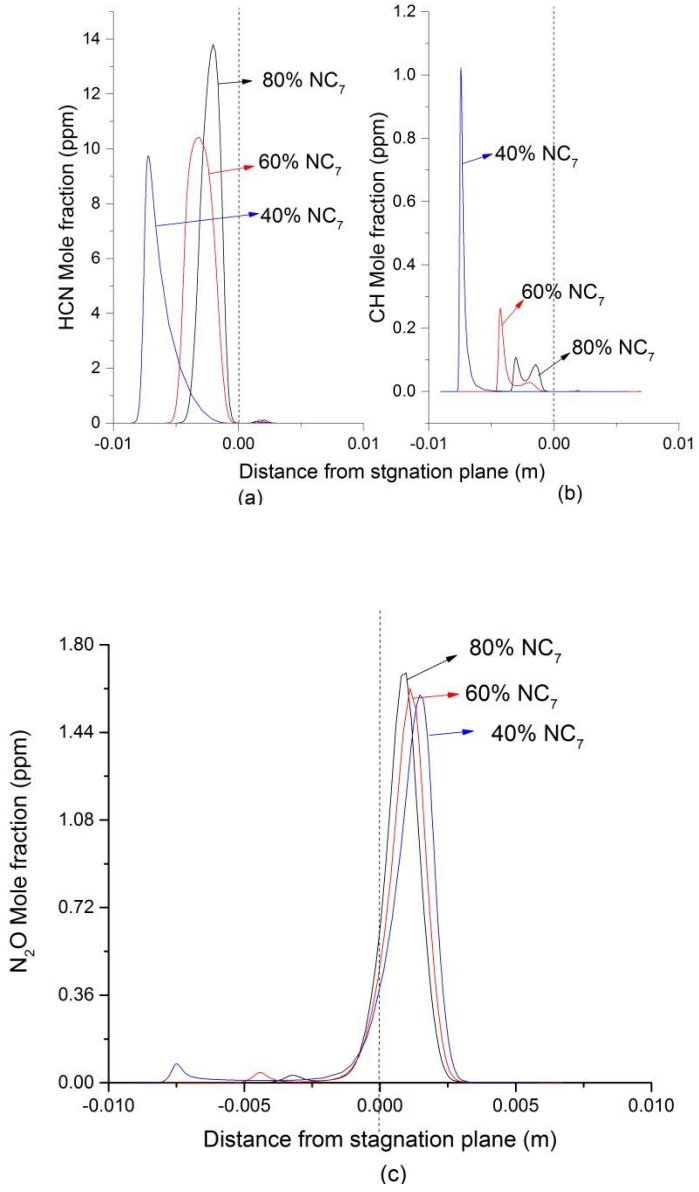

Figure 17 (a, b and c): HCN, CH, and N_2O profiles plotted with respect to the stagnation plane for three dual-fuel triple flames corresponding to 80%, 60%, and 40% energy content in n-heptane. Strain rate is 100 s^{-1}. The vertical dashed line indicates the stagnation plane.

3.4 **Effect of Fuel Blending Strategies on Emission and Thermal Efficiency**

The other part of this thesis deals with different strategies of blending methane with n-heptane and their effects on emission and thermal efficiency. As indicated in Table 4, we have examined three different fuel blending strategies in order to emulate different fuel injection scenarios in a dual-fuel engine. Strategy 1 involves the introduction of both fuels through the fuel nozzle, while in strategy 2; n-heptane is introduced from the fuel nozzle and methane from both the nozzles. In strategy 3, n-heptane and methane are introduced from the fuel and oxidizer nozzles, respectively. For all the cases, total energy flow rate into the system and the global strain rate are kept constant. Detailed results for Strategy 2 have been provided in the preceding sections. This strategy simulates conditions for a dual-fueled diesel engine in which the diesel fuel is directly injected while the natural gas is mixed with air and introduced through the intake valve. Some global results concerning the effect of three strategies on emissions and efficiency are presented in this section.

Strategy (Set) #	Fuel Side Nozzle	Oxidizer side nozzle
1	n-heptane + methane + air	Air
2	n-heptane + methane + air	Methane+ air
3	Heptane + air	Methane + air

Table 4: Different strategies for blending methane with n-heptane.

Figure 18 presents the variation of EINO with respect to n-heptane energy content for the three strategies. As indicated, the EINO values are lower for strategies 2 and 3. Results also indicate for strategies 2 and 3, an optimum fuel blend ratio corresponding to the minimum EINO. Figure 19 shows the variation of EIBENZ and thermal efficiency with respect to n-heptane energy content for the three blending strategies. As the n-heptane energy content is decreased, i.e., the amount of methane in the blend is increased, the EIBENZ decreases for all three dual-fuel strategies. However, the reduction in EIBENZ is much more pronounced for strategies 2 and 3 compared to that for strategy 1. Regarding thermal efficiency, as the n-heptane energy content is decreased, it leads to noticeable higher thermal efficiency for strategies 2 and 3. In contrast, the thermal efficiency decreases for strategy 1.

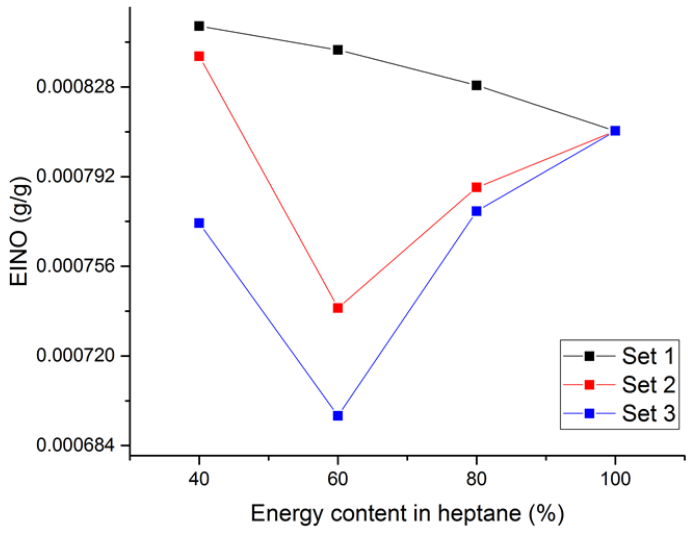

Figure 18: EINO (NO emission index) versus n-heptane energy content for the three fuel-blending strategies while keeping the total input rate fixed. The strain rate is 100 s^{-1}.

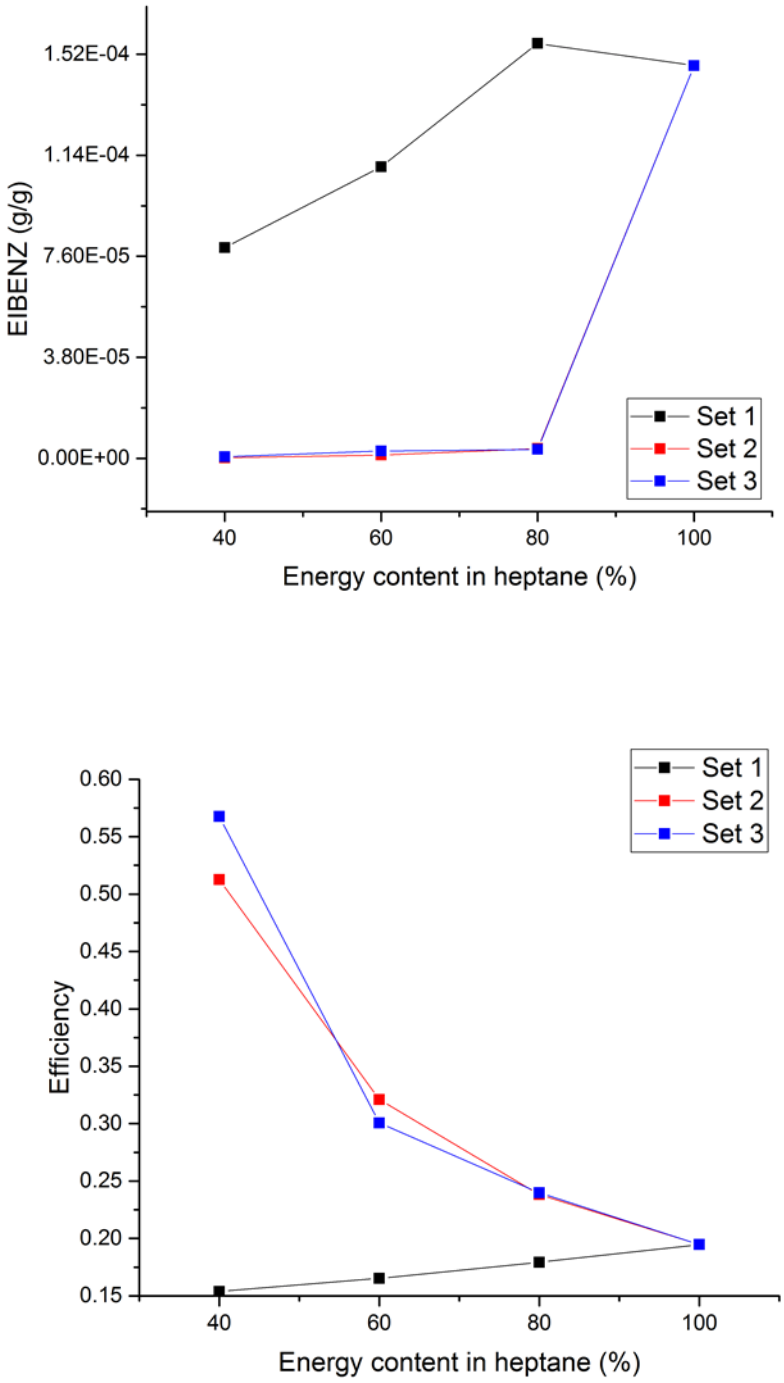

Figure 19: Variation of EIBENZ (benzene emission index) and efficiency with respect to n-heptane energy content for the three blending strategies as discussed in the context of Fig. 18.

In summary, an important observation from Figures 18 and 19 is that strategy #1 yields the highest EINO and EIBENZ and the least efficiency as compared to other two strategies, and is therefore not recommended. Note that the most significant difference between strategy #1 and other two strategies is that the flame formed with the first strategy is a double flame, whereas both strategies 2 and 3 result in a triple flame. Finally it should be noted that strategies 2 and 3 are quite comparable to each other and show almost the same trends. It can be concluded that the flame structure plays a major role in determining the emissions and efficiency.

4. CONCLUSIONS:

We have performed numerical simulations to investigate NO_x and soot emissions in n-heptane/methane triple flames in an opposed-jet configuration. A detailed fuel and NO_x chemistry model has been combined with a soot model. N-heptane and methane are considered surrogate fuels for diesel and natural gas, respectively. In order to evaluate various fuel injection scenarios in a dual-fuel diesel engine, three different strategies of blending n-heptane and methane have been examined. Strategy 1 involves the introduction of both fuels through the fuel nozzle, while in strategy 2, n-heptane is introduced from the fuel nozzle and methane from both the nozzles. In strategy 3, n-heptane and methane are introduced from the fuel and oxidizer nozzles, respectively. For each strategy, NO_x, PAH and soot emissions, and thermal efficiency are characterized by varying the relative energy content between the two fuels, while keeping the total energy input rate and strain rate fixed. Important observations are as follows.

The most important difference between blending strategy #1 and other two strategies is that the flame formed with the first strategy is a double flame, whereas strategies 2 and 3 result in a triple flame. Consequently, strategies 2 and 3 yield nearly the same trends in terms of emissions and thermal efficiency as the amount of n-heptane in the blend is varied.

The triple flame structure is characterized by three reaction zones, with the rich premixed zone (RPZ) and lean premixed zone (LPZ) located on the fuel and oxidizer sides, respectively, and the nonpremixed zone (NPZ) located near the stagnation plane. Most of prompt NO is formed in the RPZ, while thermal NO is mostly produced in the NPZ, and that due to N_2O intermediate route is formed in the LPZ. PAH species (benzene, pyrene, etc.) are formed in the RPZ, and consequently nucleation and soot formation occur between RPZ and stagnation plane,

while soot oxidation occurs on the oxidizer side of stagnation plane. As n-heptane in the blend is decreased, both the RPZ and LPZ move away from the stagnation plane, and the triple flame becomes broader.

As n-heptane in the blend is reduced, the benzene emission index (EIBENZ) and consequently soot emission decrease with all three strategies. However, the reduction is much more pronounced with strategies 2 and 3 compared to strategy 1. In addition, reducing n-heptane in the blend leads to higher thermal efficiency with strategies 2 and 3, but lower efficiency with strategy 1. With regards to NO_x emission, results indicate an optimum fuel blending ratio corresponding to a minimum EINO for strategies 2 and 3. In contrast, for strategy 1, EINO increases monotonically as n-heptane in the blend is reduced. Thus strategy #1, which yields higher NO_x, PAH and soot emissions, and lower efficiency compared to other two strategies, is not recommended.

5. REFERENCES:

[1] "Independent Petroleum Association of America (IPAA)." [Online]. Available: http://www.ipaa.org/.

[2] S. Report, "Building a stronger , safer BP Who we are," 2014.

[3] "When will oil run out? | Institution of Mechanical Engineers." [Online]. Available: http://www.imeche.org/knowledge/themes/energy/energy-supply/fossil-energy/when-will-oil-run-out.

[4] "• OPEC crude oil price change 2015 | Statistic." [Online]. Available: http://www.statista.com/statistics/262858/change-in-opec-crude-oil-prices-since-1960/.

[5] P. M. Duc and K. Wattanavichien, "Study on biogas premixed charge diesel dual fuelled engine," *Energy Convers. Manag.*, vol. 48, no. 8, pp. 2286–2308, 2007.

[6] K. Ryu, "Effects of pilot injection timing on the combustion and emissions characteristics in a diesel engine using biodiesel-CNG dual fuel," *Appl. Energy*, vol. 111, pp. 721–730, 2013.

[7] J. D. Naber, D. L. Siebers, S. S. Di Julio, and C. K. Westbrook, "Effects of natural gas composition on ignition delay under diesel conditions," *Combust. Flame*, vol. 99, no. 2, pp. 192–200, 1994.

[8] C. Abagnale, M. C. Cameretti, L. De Simio, M. Gambino, S. Iannaccone, and R. Tuccillo, "Numerical simulation and experimental test of dual fuel operated diesel engines," *Appl. Therm. Eng.*, vol. 65, no. 1–2, pp. 403–417, 2014.

[9] A. P. Carlucci, D. Laforgia, R. Saracino, and G. Toto, "Combustion and emissions control in diesel-methane dual fuel engines: The effects of methane supply method combined with variable in-cylinder charge bulk motion," *Energy Convers. Manag.*, vol. 52, no. 8–9, pp. 3004–3017, 2011.

[10] J. Liu, F. Yang, H. Wang, M. Ouyang, and S. Hao, "Effects of pilot fuel quantity on the emissions characteristics of a CNG/diesel dual fuel engine with optimized pilot injection timing," *Appl. Energy*, vol. 110, pp. 201–206, Oct. 2013.

[11] A. Shah, S. S. Thipse, A. Tyagi, S. D. Rairikar, K. P. Kavthekar, N. V. Marathe, and P. Mandloi, "Literature Review and Simulation of Dual Fuel Diesel-CNG Engines," 2011.

[12] B. B. Sahoo, N. Sahoo, and U. K. Saha, "Effect of engine parameters and type of gaseous fuel on the performance of dual-fuel gas diesel engines-A critical review," *Renewable and Sustainable Energy Reviews*, vol. 13, no. 6–7. pp. 1151–1184, 2009.

[13] S. Singh, L. Liang, S.-C. Kong, and R. D. Reitz, "Development of a Flame Propagation Model for Dual-Fuel Partially Premixed Compression Ignition Engines," *Int. J. Engine Res.*, vol. 7, no. 1, pp. 65–75, May 2006.

[14] A. L. Boehman and O. Le Corre, "Combustion of Syngas in Internal Combustion Engines," *Combust. Sci. Technol.*, vol. 180, no. 6, pp. 1193–1206, May 2008.

[15] H. Guo, F. Liu, and G. J. Smallwood, "A numerical study on NOx formation in laminar counterflow CH4/air triple flames," *Combust. Flame*, vol. 143, no. 3, pp. 282–298, 2005.

[16] A. M. Briones, S. Som, and S. Aggarwal, "Effect of multistage combustion on NOx emissions in methane-air flames," *Combust. Flame*, vol. 149, no. 4, pp. 448–462, 2007.

[17] H. Guo and G. J. Smallwood, "A numerical investigation on NOX formation in counterflow n-heptane triple flames," *Int. J. Therm. Sci.*, vol. 46, no. 9, pp. 936–943, 2007.

[18] S. K. Aggarwal, O. Awomolo, and K. Akber, "Ignition characteristics of heptane-hydrogen and heptane-methane fuel blends at elevated pressures," *Int. J. Hydrogen Energy*, vol. 36, no. 23, pp. 15392–15402, 2011.

[19] D. I. Kolaitis and M. a. Founti, "On the assumption of using ??-heptane as a 'surrogate fuel' for the description of the cool flame oxidation of diesel oil," *Proc. Combust. Inst.*, vol. 32 II, pp. 3197–3205, 2009.

[20] J. Prager, H. N. Najm, M. Valorani, and D. a. Goussis, "Structure of n-heptane/air triple flames in partially-premixed mixing layers," *Combust. Flame*, vol. 158, no. 11, pp. 2128–2144, 2011.

[21] Reaction Design, "Chemkin Theory Manual," no. September, pp. 1–386, 2010.

[22] "» Background NaturalGas.org." [Online]. Available: http://naturalgas.org/overview/background/.

[23] "Cummins Dual Fuel Engines." [Online]. Available: http://cumminsengines.com/dual-fuel.

[24] A. E. Lutz, R. J. Kee, J. F. Grcar, and F. M. Rupley, "OPPDIF: A Fortran program for computing opposed-flow diffusion flames," Albuquerque, NM, and Livermore, CA (United States), May 1997.

[25] R. Kee, J. Miller, G. Evans, and G. Dixon-Lewis, "Twenty-Second Symposium (International) on Combustion," *Combust. Institute, Pittsburgh*, 1988.

[26] B. X. Han and M. S. M. Engineering, "Effect of Unsaturated Bonds on NOx and PAH Emissions of Triple Flames," 2012.

[27] E. Ranzi, M. Dente, a. Goldaniga, G. Bozzano, and T. Faravelli, “Lumping procedures in detailed kinetic modeling of gasification, pyrolysis, partial oxidation and combustion of hydrocarbon mixtures,” *Prog. Energy Combust. Sci.*, vol. 27, no. 1, pp. 99–139, 2001.

[28] M. Bistolfi, G. Fornasari, M. Molinari, S. Palmery, M. Dente, and E. Ranzi, “Kinetic model for methane oxidative coupling reactors,” *Chem. Eng. Sci.*, vol. 47, no. 9–11, pp. 2647–2652, Jun. 1992.

[29] P. Glarborg, A. D. Jensen, and J. E. Johnsson, “Fuel nitrogen conversion in solid fuel fired systems,” *Prog. Energy Combust. Sci.*, vol. 29, no. 2, pp. 89–113, 2003.

[30] H. Guo and G. J. Smallwood, “A numerical study on the effect of CO addition on extinction limits and NO x formation in lean counterflow CH 4 /air premixed flames,” *Combust. Theory Model.*, vol. 11, no. 5, pp. 741–753, Sep. 2007.

[31] P. C. Malte and D. T. Pratt, “Measurement of atomic oxygen and nitrogen oxides in jet-stirred combustion,” *Symp. Combust.*, vol. 15, no. 1, pp. 1061–1070, Jan. 1975.

[32] J. Appel, H. Bockhorn, and M. Frenklach, “Kinetic Modeling of Soot Formation with Detailed Chemistry and Physics: Laminar Premixed Flames of C2 Hydrocarbons,” *Combust. Flame*, vol. 121, pp. 122–136, 2000.

[33] M. Frenklach and S. J. Harris, “Aerosol dynamics modeling using the method of moments,” *J. Colloid Interface Sci.*, vol. 118, no. 1, pp. 252–261, Jul. 1987.

[34] I. K. Puri and K. Seshadri, “Extinction of diffusion flames burning diluted methane and diluted propane in diluted air,” *Combustion and Flame*, vol. 65, no. 2. pp. 137–150, 1986.

[35] “Wolfram|Alpha: Computational Knowledge Engine.” [Online]. Available: http://www.wolframalpha.com/.

[36] P. Berta, S. K. Aggarwal, and I. K. Puri, “An experimental and numerical investigation of n-heptane/air counterflow partially premixed flames and emission of NOx and PAH species,” *Combust. Flame*, vol. 145, no. 4, pp. 740–764, 2006.

[37] X. Fu, S. Garner, S. K. Aggarwal, and K. Brezinsky, “A Numerical Study of NOx emissions from n-Heptane and 1-Heptene Counterflow Flames.,” *Energy & Fuels*, no. x, 2012.

[38] “Shimizu, T.; Williams, F. A.; Frassoldati, A. Proceedings of the 43rd American Institute of Aeronautics and Astronautics (AIAA) Aerospace Sciences Meeting and Exhibit; Reno, NV, Jan 10−13, 2005; AIAA-0144.”

[39] A. Frassoldati, T. Faravelli, and E. Ranzi, “Kinetic modeling of the interactions between NO and hydrocarbons at high temperature,” *Combust. Flame*, vol. 135, no. 1–2, pp. 97–112, 2003.

[40] X. Fu, X. Han, K. Brezinsky, and S. Aggarwal, “E ff ect of Fuel Molecular Structure and Premixing on Soot Emissions from n - Heptane and 1 - Heptene Flames,” 2013.

[41] S. C. Li and F. a. Williams, “NO(x) formation in two-stage methane-air flames,” *Combust. Flame*, vol. 118, no. 3, pp. 399–414, 1999.

VITA:

Name: Prithviraj P Sabnis

Education: B.E. University of Pune, India (2013)

M.S. University of Illinois at Chicago, USA (2015)